

UC San Diego

UC San Diego Electronic Theses and Dissertations

Title

Evaluating spatial variability of courtship associated sounds by Nassau Grouper (*Epinephelus striatus*) at a multi-species spawning aggregation site

Permalink

<https://escholarship.org/uc/item/9x01z33n>

Author

Van Horn, Cameron

Publication Date

2022

Peer reviewed|Thesis/dissertation

UNIVERSITY OF CALIFORNIA SAN DIEGO

Evaluating spatial variability in courtship-associated sounds of Nassau Grouper *Epinephelus striatus* at a multi-species spawning aggregation site

A Thesis submitted in partial satisfaction of the requirements
for the degree Master of Science

in

Marine Biology

by

Cameron Van Horn

Committee in charge:

Professor Brice X. Semmens, Chair
Professor Simone Bauman-Pickering
Professor Dovi Kacev

2022

Copyright

Cameron Van Horn, 2022

All rights reserved.

The Thesis of Cameron Van Horn is approved, and it is acceptable in quality and form for publication on microfilm and electronically.

University of California San Diego

2022

TABLE OF CONTENTS

Thesis Approval Page iii

Table of Contents iv

List of Figuresv

List of Tables vi

List of Abbreviations vii

Acknowledgements..... viii

Abstract of the Thesis ix

1. Introduction..... 1

2. Methods.....6

 2.1 Study Site.....6

 2.2 Data Collection6

 2.3 Data Processing.....9

 2.4 Data Analysis12

3. Results.....19

 3.1 Spatiotemporal trends23

 3.2 Model.....27

4. Discussion.....30

 4.1. Nassau Grouper calling trends.....30

 4.2. Spatial variability33

Appendix.....38

References.....41

LIST OF FIGURES

Figure 1: Little Cayman, Cayman Islands	7
Figure 2: Temporal trends of effort normalized Nassau Grouper CAS production rates across all hydrophones	24
Figure 3: Correlation matrix plot of correlations among each hydrophone pair	26
Figure 4: Linear regression of correlation coefficients against distance between hydrophone pairs in meters	27
Figure 5: Box plots of posterior predictions of the parameters (A) T_i , (B) D_i , and (C) FP_i (see 2.4 for variable descriptions)	29

LIST OF TABLES

Table 1: Data from evaluating classification of Nassau Grouper CAS by automatic (FADAR) and manual (human) efforts within all hydrophone datasets	14
Table 2: Parameters to measure accuracy and reliability of Nassau Grouper CAS classification by FADAR and human efforts, estimated using counts found in Table 1	21
Table A3: Results of Bayesian mixed effects model for modeling CAS rates by hour of day, day of spawning period, and fish proximity to a given hydrophone	39

LIST OF ABBREVIATIONS

PAM	Passive acoustic monitoring
CAS	Courtship associated sounds
FSA	Fish spawning aggregation
FADAR	Fish Acoustic Detection Algorithm Research
CI-DoE	Cayman Islands Department of the Environment
GMP	Grouper Moon Project
REEF	Reef Environmental Education Foundation
LARS	Loggerhead LARS-HF
ST	SoundTrap Model 300HF
LSTM	Long short-term memory
TOD	Time of day
DAFS	Days after first spawn
FP	Fish proximity
MCMC	Markov Chain Monte Carlo
FNR	False Negative Rate
TPR	True Positive Rate
FPR	False Positive Rate
WAIC	Widely Applicable Information Criterion

ACKNOWLEDGEMENTS

This body of work and the long road that led to it is anything but an individual effort. I owe immense gratitude to Brice Semmens who provided me this opportunity to conduct meaningful science with a species as wonderfully interesting as the Nassau Grouper. His entrustment of this data with me as well as the many hours of help, and an ever-present calm, jesting demeanor are things I will be forever grateful for and carry throughout my career. Thank you to Simone Baumann-Pickering and Dovi Kacev for agreeing to serve (longer than I let on) on my committee and provide necessary blunt advice in their fields of acoustics and statistics, and for encouraging me to always have space to breathe. To my lab mates in the Semmens Lab, thank you for serving as an ever-present model of work ethic and comradery, and assisting my ending efforts to get this project over the finish line. My time here at Scripps would not be possible without the tremendous encouragement and support from my parents, who never ceased to prioritize my education and assist my every effort in achieving this goal. They, my family, and friends gave me the greatest support group I could have asked for to persevere through this project. Kaito, Juan, Komal, Ethan, Charlie, Tiff, Sammy, thank you for bearing through my incessant talks, rants, and moments of self-doubt. Kendall, Canyon, and Ryan, thank you for your friendship and solidarity throughout this experience that we shared, I am incredibly fortunate to have had you three in our cohort and look forward to seeing the incredible science and contributions you all will excel through. To the innumerable others who encouraged me along the way, thank you for giving me a space outside of this work to look forward to when I could not continue to work. This paper is a testament to all of your belief in me, and the love that I reflect back to each of you over and over again.

ABSTRACT OF THE THESIS

Evaluating spatial variability in courtship-associated sounds of Nassau Grouper *Epinephelus striatus* at a multi-species spawning aggregation site

by

Cameron Van Horn

Master of Science in Marine Biology

University of California San Diego, 2022

Professor Brice X. Semmens, Chair

Passive acoustic monitoring (PAM) is a cost-effective, minimally invasive technique commonly used to study behavior and population dynamics of soniferous fish species. To understand the strengths and limitations of PAM for this purpose requires an assessment of the variability in courtship-associated sounds (CAS) as a function of time, space, and proximity for spawning fishes of interest. Here we evaluate temporal and spatial trends in CAS by Nassau Groupers (*Epinephelus striatus*) using an array of six hydrophones deployed at a large Nassau Grouper fish spawning aggregation (FSA) on Little Cayman, Cayman Islands. We collected

continuous data for nine days during a winter spawning season, and subsequently employed an automatic classifier to extract the embedded Nassau Grouper CAS. Using these data, we qualitatively and quantitatively analyzed variability in temporal trends across the spatial array with a Bayesian mixed effects model. We found a clear degradation in accuracy of temporal calling patterns at the FSA as distance from the spawning site increased, and observed higher correlations in CAS rates among the most proximal hydrophone pairs than the most separated pairs. Our model predicted strong effects of fish proximity, spawning behavior, and crepuscular periods on detected calling rates of Nassau Grouper that corroborate with and add to the present literature. Our findings suggest a high degree of variability within relatively short distances from a sonic target, thus imploring a need for better spatial resolution in acoustic analyses.

1. Introduction

Marine fisheries are globally important in the context of economic stability (US\$164B in export value), societal function (260 million jobs), and food security (17% of total animal protein consumed globally), the latter of which is considerably important in tropical and subtropical coastal communities (Milich 1999, Teh & Sumaila 2013, Worm & Branch 2012, FAO 2020). Government actions to sustain fishery productivity, such as intensive fishery-independent at-sea surveys, are often more financially limited in these regions than those of industrialized nations. These fisheries thus operate in data-poor conditions that threaten the ability to sustain catch over time. Because of this, there is a need to develop and employ cost-effective tools for monitoring populations that will allow for informed management action. In these lower latitudes, many targeted fish species in need of cheap monitoring methods are those that form highly dense and predictable fish spawning aggregations (FSAs).

FSAs, or mass gatherings of fish for reproductive purposes, recruit individuals from potentially hundreds of miles away and occur over very short annual time scales (Domeier & Colin 1997). Species that form FSAs typically do so to maximize their reproductive fitness. However, because these events are often highly predictable in space and time, aggregating populations can be intensively fished once discovered, which in turn can lead to overexploitation and ultimately collapse of the fishery. More than half of all documented FSAs in the tropical West Atlantic no longer form (Sadovy de Mitcheson et al. 2008). But because FSAs concentrate the entire reproductive biomass of a region into relatively small areas at predictable times, they present an opportunity to census stocks for the purposes of assessing health, recruitment, and recovery in depleted populations. To do so, however, requires monitoring tools that are effective,

low cost, and that can function in underwater environments that are otherwise difficult to access by researchers.

Passive acoustic monitoring (PAM), a widely used tool in bioacoustic research, is a rapidly growing technique for monitoring FSAs (Lindseth and Lobel 2018). Commonly used to study terrestrial species such as birds, bats, and insects (Laiolo 2010), PAM has been applied to a diverse range of marine soundscape projects. PAM lends itself to FSA monitoring because many species that form FSAs produce courtship-associated sounds (CAS) while aggregating (Rowell et al. 2017). Fish produce CAS to recognize conspecifics and signal mating readiness, thereby serving as a mechanism for sexual selection and reproduction (Lobel 1992, Webb et al. 2008). When actively acoustic fishes form FSAs, the CAS frequencies at these sites generally scale with density, a phenomenon that when quantified can be used to estimate fish abundance for the purpose of fisheries management (Rowell et al. 2012, 2017, Scharer et al. 2012, Sanchez et al. 2017, Caiger et al. 2020, Looby et al. 2022). Monitoring FSAs with acoustic instruments has the potential to enable CAS data collection without temporal restrictions often associated with visual fish survey methods, and it can be applied to environments in which visual monitoring is difficult (Rountree et al. 2006, Luczkovich et al. 2008, Marques et al. 2013). Furthermore, visual methods such as underwater visual census (UVC) or diver operated video (DOV) can be invasive to the target environment and affect estimates of biodiversity and abundance (Emslie et al. 2018).

While PAM presents a minimally invasive strategy to monitoring FSAs, challenges remain, including (1) the need for time-intensive classification of CAS from recordings, and (2) a poor understanding of the relationship between CAS frequency and the proximity/abundance of fish in relation to the recorder. The plethora of recorded acoustic data can pose a significant problem for timely analysis because of the inherent necessity to detect acoustic signatures, which

is often done by hand (Aalbers and Sepulveda 2012, Scharer et al. 2012, Rowell et al. 2012). Advancements in the field of machine learning algorithms have produced novel solutions in the form of automatic classifiers (Stowell et al. 2019, Munger et al. 2022). Rapid automatic classification enables large swaths of raw acoustic data to be analyzed for specific spectral signatures in a fraction of the time, and has been applied to fish species such as Atlantic cod (*Gadus morhua*) and several Sciaenids (Caiger et al. 2020, Monczak et al. 2019). For grouper species that form FSAs in the tropical Western Atlantic, Ibrahim et al. (2018) developed FADAR (Fish Acoustic Detection Algorithm Research), an automatic classifier designed to detect spectral signatures of CAS. To date, however, the performance of FADAR across differing FSA locations and recording hardware remains largely untested.

Rapid automatic classification of CAS expands the potential for PAM, however a poor understanding of how CAS detections vary in space and time persists. The accuracy of passive acoustic data relies on successful transmission of an acoustic signal by a source to a recorder, the likelihood of which is high if the fish calls near the hydrophone. The spectral features of a CAS dictate its detectable range; however, this range is not likely to be known for a target species given the large paucity of studies into sound-producing fishes (Looby et al. 2022). Because passive acoustic methods often deploy a single hydrophone to monitor a population, inherent fish movement can leave the hydrophone beyond the CAS detection range. While the high spatiotemporal predictability of FSAs may warrant dismissal of these concerns, observed shifts in the specific GPS of spawning fish at several FSAs across years suggests reliance on past FSA geolocations can also risk accuracy of the data (Colin 1992, Aguilar-Perera 2006, Caiger et al. 2020). Understanding the spatial and temporal variability of CAS detections is therefore important for passive acoustic methods, though this has not been explored in the literature. We

attempt to resolve this knowledge gap by studying spatiotemporal trends in CAS production by a well-studied species known to form FSAs.

The Nassau Grouper (*Epinephelus striatus*) is a gonochoristic large-bodied opportunistic predator whose commercial, cultural, and ecological value have been known throughout the Caribbean for generations (Smith 1972, Colin 1992, Domeier & Colin 1997, Sadovy & Eklund 1999). Nassau Grouper are a long-lived, highly fecund, and late-maturing species that form transient FSAs near shelf edges (Winemiller & Rose 1992, Domeier & Colin 1997, Sadovy & Eklund 1999). Individuals demonstrate strong fidelity to the reef at which they aggregate and reproduce, a behavior perhaps socially transmitted from older, experienced fish (Bolden 2000, Semmens et al. 2007, Starr et al. 2007, Nemeth 2012, Dahlgren et al. 2016, Blincow et al. 2020). Migration to the FSA occurs around the winter full moons in the central Caribbean, where Nassau Grouper densities drastically increase and spawning behavior (stark coloration shifts and following, circling movements) is observed soon after (Smith 1972, Colin 1992, Sadovy & Eklund 1999, Starr et al. 2007, Archer et al. 2012).

Nassau Grouper are listed as Critically Endangered by the International Union for the Conservation of Nature and Natural Resources due to overfishing at FSAs throughout its historic range (Sadovy & Eklund 1999, Sadovy de Mitcheson et al. 2008, Sadovy et al. 2018). Perhaps the most well documented collapse, and subsequent recovery, of the species occurred in the Cayman Islands, a small island nation to the Southwest of Cuba. In 1986, local fishermen reported noticeable declines in Nassau Grouper catch, prompting the Cayman Islands Department of the Environment (CI-DoE) to begin monitoring the known FSAs of the species. By 2001, ongoing heavy catch at the last remaining FSA of the species (off the west end of Little Cayman) motivated the Cayman Islands government to implement an Alternate Year Fishing

Law in 2002 alongside other protective measures surrounding Nassau Grouper reproduction. By 2004, all known FSAs throughout the Caymans were protected by an 8-year fishing ban (Bush et al. 2006). Continued efforts to conserve and monitor Nassau Grouper populations have proven fruitful, as recovery has been observed at FSAs off Little Cayman and Cayman Brac (Heppell et al. 2012, Waterhouse et al. 2020, Stock et al. 2021).

Here we present a case study on spatio-temporal distribution of Nassau Grouper CAS across the west end Little Cayman FSA site during the winter spawning season in 2020. The acoustic, behavioral and reproductive ecology of Nassau Grouper at this FSA site is part of an ongoing monitoring program (The Grouper Moon Project; GMP), and thus lends itself to an intensive acoustic survey under known conditions of fish presence, spatial distribution, and reproductive behaviors. Using an array of 6 simultaneously recording hydrophones, we recorded the FSA soundscape over a 9-day period, and subsequently parsed the recordings through the FADAR CAS classifier. With the derived CAS counts from the classifier, we compare spatial distributions of averaged hourly CAS detection rates through qualitative and quantitative methods to determine the spatial synchrony/asynchrony in CAS patterns at locations across the FSA. Lastly, we assess drivers of variability in CAS by using a mixed effects model of Nassau Grouper CAS detections as a function of variables presumed to affect calling behavior (e.g. time of day, day of spawning season, location of aggregating fish relative to the hydrophone). Collectively, these analyses provide an assessment of the spatial, temporal and biological factors outside fish abundance that influence hydrophone specific CAS detection rates.

2. Methods

2.1 Study Site

The Cayman Islands hosts a large FSA of Nassau Grouper off the west end of Little Cayman (Figure 1B), and has been the target of numerous projects studying the ecology and recovery of Nassau Grouper populations (Whaylen et al. 2004, 2007; Heppell et al. 2009, 2012; Waterhouse et al. 2020; Stock et al. 2021). Much of the research in this region (including this paper) has been conducted at the west end Little Cayman FSA site by GMP, a collaborative group of researchers from the CI-DoE and Reef Environmental Education Foundation (REEF). GMP has had a profound impact on the protection efforts for the species as demonstrated by recent findings of stock recovery in some local populations. As of 2016, conservation measures by the CI-DoE include: no-take zones covering 45% of total shelf area, seasonal closures on all Nassau harvest from December 1 to April 31, and strict take and gear restrictions in open season (Waterhouse et al. 2020).

2.2 Data Collection

Hydrophone Array Deployment

To monitor Nassau Grouper CAS across the spawning site, we deployed a six-hydrophone linear array along the western shelf edge of Little Cayman from February 8 to February 17, 2020 (Figure 1C). This time period generally reflects the average residence time of Nassau Grouper at aggregation sites (Starr et al. 2007, Archer et al. 2012), with the full moon observed on February 9, 2020. Divers stationed the hydrophones in a linear path along the shelf edge at roughly 30 m depth with a 150 m distance between each (estimated by divers towing a

150 m line between deployments). At a subset of hydrophone stations, divers deployed surface marker buoys (SMBs) and a surface support team used a Garmin Etrex 20x GPS to geolocate the stations. We subsequently estimated the coordinates of the remaining stations using GPS waypoints taken at drop points of the diver teams and known distances between stations.

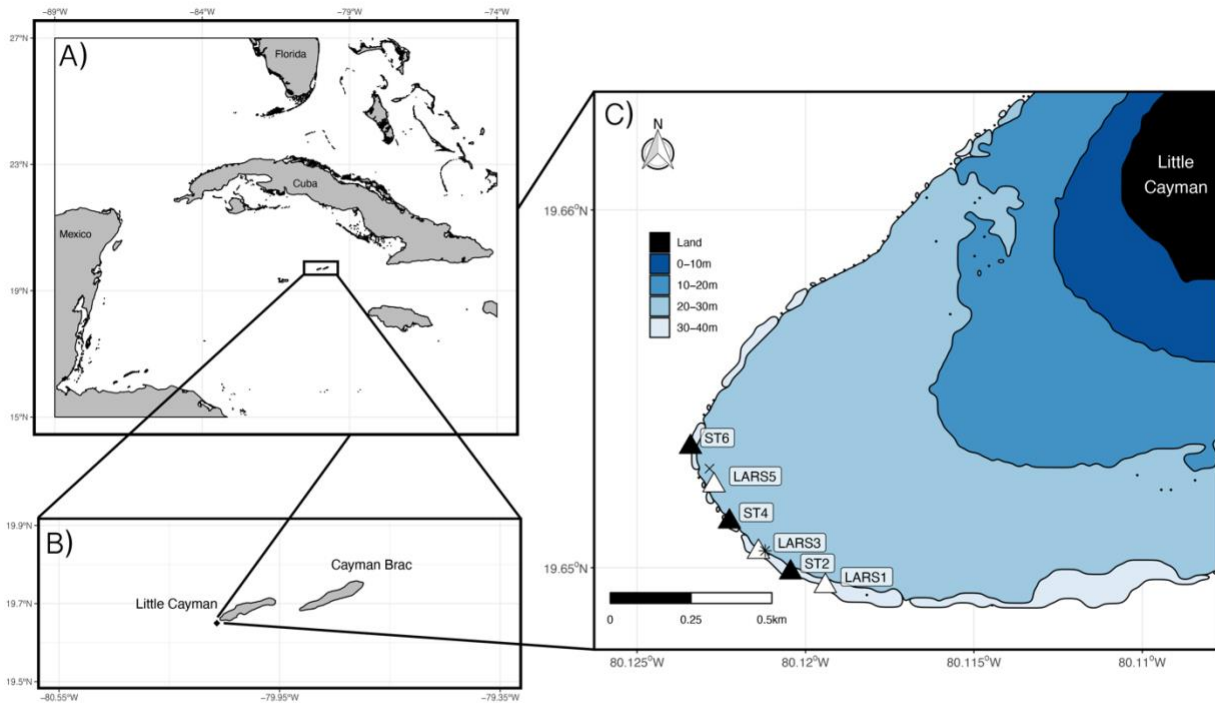


Figure 1: Little Cayman, Cayman Islands. (A) The Cayman Islands in the Caribbean Sea relative to Cuba, Florida, U.S., and Mexico. Grand Cayman, the largest island in the Caymans, is just southwest of the drawn black box. (B) Little Cayman and Cayman Brac. A black diamond off Little Cayman’s west end signifies the FSA location. (C) Bathymetry of the west end of Little Cayman. Blues lighten to symbolize increasing depth on the order of 10 meters, with land represented in black. A black ‘X’ marks the FSA observed by divers, and a black ‘*’ marks the traditional FSA location. Triangles represent hydrophones and are labeled with their station. Black triangles signify ST hydrophones and white triangles represent LARS hydrophones.

We used two brands of low-cost, long-lasting passive acoustic recorders to comprise the array: Loggerhead LARS-HF (LARS) and Ocean Instruments SoundTrap Model 300HF (ST). We alternated the model at each station along our array (Figure 1C). STs recorded continuously at a sample rate of 48kHz with high preamp gain and no high pass filter. LARSs recorded

continuously at a sample rate of 192 kHz and a sensitivity of -170 dB with no high pass filter. Audio was captured onto 256 GB memory cards as 16-bit .wav files of six-hour and one-minute increments for STs and LARSs, respectively, with date and time upon recording embedded within each file name. We stationed the hydrophones between 09:00-10:00 on February 8 and retrieved them the morning of February 17 between 09:00-10:00 (these and all times listed throughout are in Eastern Standard Time, the local time of the Cayman Islands).

GoPro Camera Deployments

To estimate Nassau Grouper presence and movement around the FSA, divers stationed GoPro HERO3 White cameras opportunistically along the array throughout the study period (LARS1 omitted). To extend battery life, we installed CamDo TL-004 intervalometers into the extra battery slot of the GoPros and programmed it to turn on and record for 2 minutes every 18 minutes. Beginning at ST2, divers opportunistically retrieved and redeployed the GoPros multiple times each day, repositioning the cameras nearest to where the fish were observed. Six GoPros were used in total with no more than two at a given station. Divers installed the GoPros within several meters of a given hydrophone on the reef bed with non-uniform angle positioning (i.e. some faced parallel to the floor while others faced upward around a 45° incline). In instances where a station had two GoPros, the cameras were positioned on different parts of the adjacent reef angled opposite each other for a better composite image.

Video Transects of the FSA

We opportunistically collected video transects of the FSA when fish schooled into a band along the shelf edge. To collect a video transect, a diver used a Canon 1DX mark ii – Sigma 18-

35mm f/1.8 Lens – Nauticam Wide Angle Conversion Port (WACP) and a Dive X Piranha P1 Scooter to traverse the length of the band while keeping aggregating fish within the camera frame. Divers collected video censuses during multiple dives throughout the spawning period. We examined each video census to determine (1) the daily/hourly locations of the band of fish at the spawning site, and (2) where the fish were most abundant during each dive using underwater visible landmarks and marking buoys.

In Situ Diver Observations

Researchers conducted 3 dives each day in the morning, afternoon, and evening with exceptions on the first, penultimate, and final days of hydrophone data collection. Divers noted fish location, presence, abundance, and movement around the spawning site. For spatial accuracy, divers approximated fish position and movement using established moorings, landmarks, and stations along the shelf edge. These *in situ* diver observations, in concert with GoPro recordings and video transects, were later used to approximate the coordinates for the bulk of the aggregating fish, as well as estimated northern and southern boundary limits of the FSA.

2.3 Data Processing

Hydrophone Array

To analyze spatial variability of Nassau Grouper CAS during the recording period, the large volume of data generated by PAM required a standardization effort to produce CAS frequencies per hour for each hydrophone. We began this process by considering differences in data generation by each hydrophone model and instances of sonic intrusion by loud

anthropogenic sources. We segmented the acoustic data from ST hydrophones, initially recorded in six-hour lengths, into one-minute intervals to facilitate temporal comparisons with the automatically segmented LARS data.

Boats frequented the aggregation site during recording, creating low-frequency interference at sporadic intervals. While daily research dive operations constituted most of this boat traffic, small local fishing vessels periodically visited the site in the morning while fishing for tuna just off the shelf. The frequency range of vessel noise overlaps with Nassau Grouper CAS and masks detections while present. Also, we found that FADAR confused some instances of low-frequency anthropogenic noise with Nassau Grouper calls and overestimated CAS counts therein. For these reasons, we removed all segmented acoustic data containing vessel noise from our analysis. Because we recorded over 1,000 hours of the FSA soundscape, the likelihood of encountering anthropogenic noise in any given minute was low. To efficiently identify instances of vessel interference at all hydrophones, we subset each dataset to represent 1 minute for every 5 recorded minutes. We then ingested the subset recordings into Audacity 2.4.2 to visually inspect the spectrograms for anthropogenic noise. We defined minutes as containing interference if at least half of the file's length contained anthropogenic noise between frequencies of 0-600 Hz. Because we did not inspect every minute recorded, we assumed identified instances of interference also occurred 2 minutes prior to and after the observed instance. After cleaning the data of anthropogenic noise, we tracked minutes annotated within all hours at each hydrophone to normalize CAS detections per hour by annotation effort.

Call Classification

The spectral qualities and statistics of Nassau Grouper CAS are well known (Scharer et al. 2012, Rowell et al. 2018, Wilson et al. 2020). Because of the volume of acoustic data generated in our study, we used a combination of automatic CAS classification using the FADAR software (Ibrahim et al. 2018) and manual classification. Nassau Groupers have three unique identified CAS, and a hypothesized fourth CAS by Wilson et al. (2020) that we did not include in this study because FADAR has not been trained to detect it at present. In agonistic encounters, Nassau Grouper often produce a sequence of individual pulse sounds (termed pulse trains). The individual pulse segments last on the order of 0.09 ± 0.02 s while the full train can last up to 3 s, and has a peak frequency of 77.4 ± 30.3 Hz (Scharer et al. 2012, Wilson et al. 2020). During courtship, Nassau Grouper emit a low-frequency tonal sound that lasts 1.6 ± 0.3 s and has a peak frequency of 99.0 ± 33.6 Hz (Scharer et al. 2012). Lastly, Rowell et al. (2018) identified a third Nassau Grouper CAS described as akin to that of a heartbeat. The CAS has properties similar to the pulse train, with a mean duration of 0.37 s and mean peak frequency of 117.7 Hz (Rowell et al. 2018). FADAR does not specify which Nassau CAS it detects, thus the CAS counts in this study are nonspecific.

FADAR operates by ingesting an acoustic signal and (1) denoising the signal through discrete wavelet transformation, (2) processing the signal through long short-term memory (LSTM) layered networks, and (3) attributing discriminative features of the signal for final classification of the origin species. FADAR divides the time series of the acoustic spectra into signals of 2-second lengths. Each of these 2-second bins can only have 1 attributable CAS, if any, regardless of species. The classifier sums CAS detections and links their associated 2-second bins within each audio file (e.g. a CAS detected at seconds 33-37 will be noted as 1 CAS occurring between seconds 32-38).

2.4 Data Analysis

Confusion matrices

To assess FADAR’s automatic classification performance, we developed confusion matrices and calculated relevant estimates of accuracy indices. First, we randomly sampled 200 minutes of recordings from each hydrophone for analysis in FADAR. We then had a trained researcher listen to the acoustic samples in Audacity to identify instances of Nassau Grouper CAS. To prevent any bias in our evaluation of FADAR, we enumerated CAS along the same constraints as that of the classifier. Specifically, FADAR assigns time stamps to detected CAS by dividing the acoustic time series into bins of 2-second lengths and assigning no more than 1 CAS to each bin. This method may prevent FADAR from, for instance, detecting a short tonal CAS that occurs within the same 2-second bin as a proximal pulse CAS. We therefore required the trained researcher doing manual CAS identification to provide time stamps in intervals of 2-seconds for all identified CAS and barred any given CAS from temporally overlapping with another CAS. We termed detections heard by the human researcher as ‘true’ CAS and FADAR as ‘predicted’ CAS. The comparison of these two metrics forms confusion matrices: true positives (agreed presence), true negatives (agreed absence), false positives (predicted presence that was absent) and false negatives (predicted absence that was present). FADAR predicts if CAS are present in 2-second windows, thus in each minute (the length of an analyzed file) the classifier makes 30 predictions. Because CAS presence is a relatively rare event, many of these predictions are likely to be true negatives, adding positive bias in accuracy estimates of FADAR. Therefore, we defined true negatives as full minutes with no detected or present CAS. When we sampled 200 minutes from each hydrophone, the subsets from LARS1 and ST6 yielded

substantially fewer CAS detections (regardless of method) relative to ST2, ST4, and LARS5. We therefore added additional random draws to the test datasets of these hydrophones to meet a minimum threshold of 100 ‘true’ CAS present in test data.

We calculated the following statistics for all confusion matrices: accuracy, misclassification rate, rates for all true/false positive/negative terms, precision, prevalence, null error, and Cohen’s Kappa. Variables to inform all evaluative statistics included the four true/false positive/negative terms along with summed values for predicted positives, predicted negatives, actual positives, actual negatives, and total detections (present and absent). Equations to relate these parameters to the above statistics can be found in the appendix.

FADAR performed poorly within ST2 and ST4s datasets (Table 1 & 2), prompting a subsequent manual (human) classification effort for all the data from these hydrophones. Because these datasets contained nearly 26,000 cumulative minutes, we subset the data to represent 1 minute for every 5 minutes of recording (identical to that of the anthropogenic parsing effort in 2.3). We ingested the acoustic .wav files into Audacity to visualize the acoustic spectra for CAS identification and restricted observable frequencies between 0 and 600 Hz, with 20 dB gain and a range of 80 dB. We used a frequencies algorithm with a Hamming window size of 16384 and a zero-padding factor of 1. To maintain consistency among CAS extraction in all hydrophones, we mimicked FADAR’s execution by enumerating CAS solely through visual identification in spectrograms. We also similarly confined detected CAS to 2 s windows with no more than one CAS detection per window.

We evaluated the human classification effort identically to that of FADAR. We defined visually detected CAS as ‘predicted’ and audial CAS detections as ‘true’. Upon confirming that the human effort compared well with that of FADAR, we proceeded with analysis.

Table 1: Data from evaluating classification of Nassau Grouper CAS by automatic (FADAR) and manual (human) efforts within all hydrophone datasets. Only ST2 and ST4 required human evaluation due to poor performance by FADAR within their respective datasets.

Station	Classifier	Sample Size	n	True Positive	True Negative	False Positive	False Negative	Actual Presence	Actual Absence	Predicted Presence	Predicted Absence
LARS1	FADAR	294	317	64	215	1	37	101	216	65	252
	HUMAN	200	185	15	76	0	94	109	76	15	170
ST2	FADAR	200	271	131	96	17	27	158	113	148	123
	HUMAN	200	275	5	161	0	109	114	161	5	270
ST4	FADAR	200	309	173	87	9	40	213	96	182	127
	HUMAN	200	337	204	80	10	48	252	90	214	128
LARS5	FADAR	235	307	90	170	3	44	134	173	93	214

GoPro and diver observations

We sought to categorize the proximity of the bulk of Nassau Groupers to each hydrophone for all recorded hours. To do this, we gathered visual census data from simultaneous GoPro recordings and observations of fish presence and movement from dive logs. We inspected all GoPro files to categorize Nassau Grouper abundances per hour into one of five categories: absent (0), individual (1), few (2), many (3), and abundant (4). Because individuals would swim in and out of the camera's view, we categorized abundances based on the greatest observed density of Nassau Grouper (i.e. if a large school of Nassau was only visible at the end of the recording, the assigned category would be 'many' or 'abundant' depending on the size of the school).

While GoPro data reflected observable Nassau Grouper abundances, limitations with respect to light and resources presented challenges that restricted cameras to observe no more than two hydrophones at a time during hours of adequate sunlight. Dive logs and video pans conducted multiple times daily provided supplementary abundance estimates and Nassau presences. Divers recorded Nassau behavior, movement, and relative proximity to nearest hydrophones using unique landmark and mooring descriptors for high spatial resolution. We used these diver observations to estimate where fish moved around the array for all recorded daylight hours as well as their abundances at hydrophones not observed by GoPros. We then combined the estimated position and relative abundances of Nassau Groupers from dive logs with the categorized abundances from the GoPro data to create proximities of Nassau Groupers to each hydrophone for all observable hours. We divided these proximities into three categories: not observed (0), where neither divers nor GoPros observed fish within 100 meters of the hydrophone; nearby (1), where GoPros or divers observed fish within 100 meters of the

hydrophone; and present (2), where GoPros or divers observed fish within 20 meters of the hydrophone.

Correlation

Before modeling CAS as a function of time and space covariates (see below), we calculated simple correlations of detected CAS per hour among hydrophone pairs and compared the coefficient rho (ρ) to distances between each pair. Predicted Nassau Grouper CAS were summed per hour at each hydrophone for all hours in the study period and normalized by observation effort within each hour. Several sporadic hours contained no observable minutes of CAS, and were removed from the dataset. Further, due to an anomalous error at ST4 that halted recording, only data prior to February 15 was included. We calculated distances between pairs of hydrophones from their estimated coordinate data using the ‘geosphere’ package in R. Correlation matrices and their respective 95% confidence intervals were calculated using the ‘corrplot’ package in R.

Model

Because we are interested in the spatiotemporal variability of CAS, we used the number of detected CAS for hydrophone j at time interval i of the study (V_{ij}) as a Poisson distributed response variable in a Bayesian hierarchical modeling framework:

$$V_{j,i} \sim \text{Poisson}(\lambda)$$

$$\log \lambda_{j,i} = (T_i + D_i + FP_i + h_{j,i}) * m_{j,i}/60$$

$$\begin{bmatrix} h_{1,i} \\ h_{2,i} \\ h_{3,i} \\ h_{4,i} \\ h_{5,i} \end{bmatrix} \sim \text{MVNormal} \left(\begin{pmatrix} 0 \\ 0 \\ 0 \\ 0 \\ 0 \end{pmatrix}, \mathbf{S}_H \right)$$

$$\mathbf{S}_H = \begin{pmatrix} \sigma_{h1} & 0 & 0 & 0 & 0 \\ 0 & \sigma_{h2} & 0 & 0 & 0 \\ 0 & 0 & \sigma_{h3} & 0 & 0 \\ 0 & 0 & 0 & \sigma_{h4} & 0 \\ 0 & 0 & 0 & 0 & \sigma_{h5} \end{pmatrix} \mathbf{R} \begin{pmatrix} 1 & \rho_{1,2} & \rho_{1,3} & \rho_{1,4} & \rho_{1,5} \\ \rho_{2,1} & 1 & \rho_{2,3} & \rho_{2,4} & \rho_{2,5} \\ \rho_{3,1} & \rho_{3,2} & 1 & \rho_{1,2} & \rho_{3,5} \\ \rho_{4,1} & \rho_{4,2} & \rho_{4,3} & 1 & \rho_{4,5} \\ \rho_{5,1} & \rho_{5,2} & \rho_{5,3} & \rho_{5,4} & 1 \end{pmatrix}$$

$$T_j \sim \text{Normal}(0,1)$$

$$D_j \sim \text{Normal}(0,1)$$

$$FP_j \sim \text{Normal}(0,1)$$

$$\sigma_d \sim \text{Exponential}(1)$$

$$\mathbf{R} \sim \text{LKJcorr}(8)$$

In the above model formulation, the number of CAS detected at a given hydrophone and hour is a function of time of day (24 categories reflecting hour of day; T_i), day of the spawning season relative to night of first spawn (7 categories reflecting -4 to +2 days after first spawn DAFS; D_i), proximity of the bulk of spawning fish relative to each hydrophone (categorical estimate with 3 levels; FP_i), and a random effect of recording time interval (each hour of the study; $h_{j,i}$). We define these $h_{j,i}$ values to be multivariate normal within each time interval in order to account for the expected correlated nature of CAS detections between hydrophones related to the spatial nature of fish behaviors and CAS at the spawning site. Within the covariance structure (\mathbf{S}_H), each hydrophone has a separate variance, while the covariance of hydrophones (\mathbf{R}) is assumed to be fixed across hours. That is, we expected limited hydrophone detection ranges coupled with complex aggregating behaviors (e.g., dispersing from or coalescing to a specific location within the array as a function of time of day or ocean condition) would lead to correlations in CAS

detections across hydrophones that would not be captured simply by the proximity of spawning fish to each hydrophone independently.

We confined time intervals to hour segments across the entire study period. In some instances, a hydrophone only recorded a portion of a given hour interval, defined as $m_{j,i}$ (the number of minutes per hour recorded). To address these disparities, we standardized the expected CAS value for each $V_{j,i}$ by including the term $m_{j,i}/60$.

We specified weakly regularizing priors for all priors in our model formulation above and fit the model using STAN (Stan Development Team 2022) via the `ulam` function in the Statistical Rethinking R package (McElreath R 2020). We ran four chains concurrently with 10000 iterations per chain, and evaluated convergence based on trace plots and Gelman-Rubin scores (all parameters ~ 1 , indicating efficient mixing among MCMC chains and model convergence). All data and model code used in our analysis are available at <https://github.com/cjvanhorn>.

3. Results

Most hydrophones in the deployed array recorded for the duration of the study period. However, LARS3 malfunctioned early in the recording period and did not gather sufficient data for analysis. In addition, ST4 abruptly ended its recording near midnight on February 15, two days prior to the end of the study period. Despite these issues, we collected over 1000 hours of acoustic data. Classifications from FADAR had an overall accuracy of 76.0%, and an associated Cohen's Kappa (K) estimate of 51.4. The software also produced an inflated false negative rate (FNR) of 46.8% and a low true positive rate (TPR, or recall) of 53.2%. However, an investigation into the classifier's performance for each hydrophone indicated particularly poor performance within ST2 and ST4. Upon removing ST2 and ST4 samples from the cumulative

subset, FADARs performance improved considerably. Summed samples from LARS1, LARS5, and ST6 generated a high accuracy of 85.6%, high recall of 73.5%, low FNR of 26.5%, and a K of 70.5. FADAR yielded a low average false positive rate (FPR) of 2.0% for all stations, with the well-performing stations (LARS1, LARS5, and ST6) yielding a comparable average of 2.9%.

Because of FADAR's relatively poor performance on stations ST2 and ST4, we used manual classification. Manual classification accuracy was comparable to that of FADAR, and performed better with higher recall and lower FNR; however, it also yielded poorer specificity and FPR, with a marginally lower K. Manual classification within stations ST2 and ST4 were highly comparable to each other, suggesting no bias within either sample.

Table 2: Parameters to measure accuracy and reliability of Nassau Grouper CAS classification by FADAR and human efforts, estimated using counts found in Table 1. Equations to calculate each parameter can be found in the appendix.

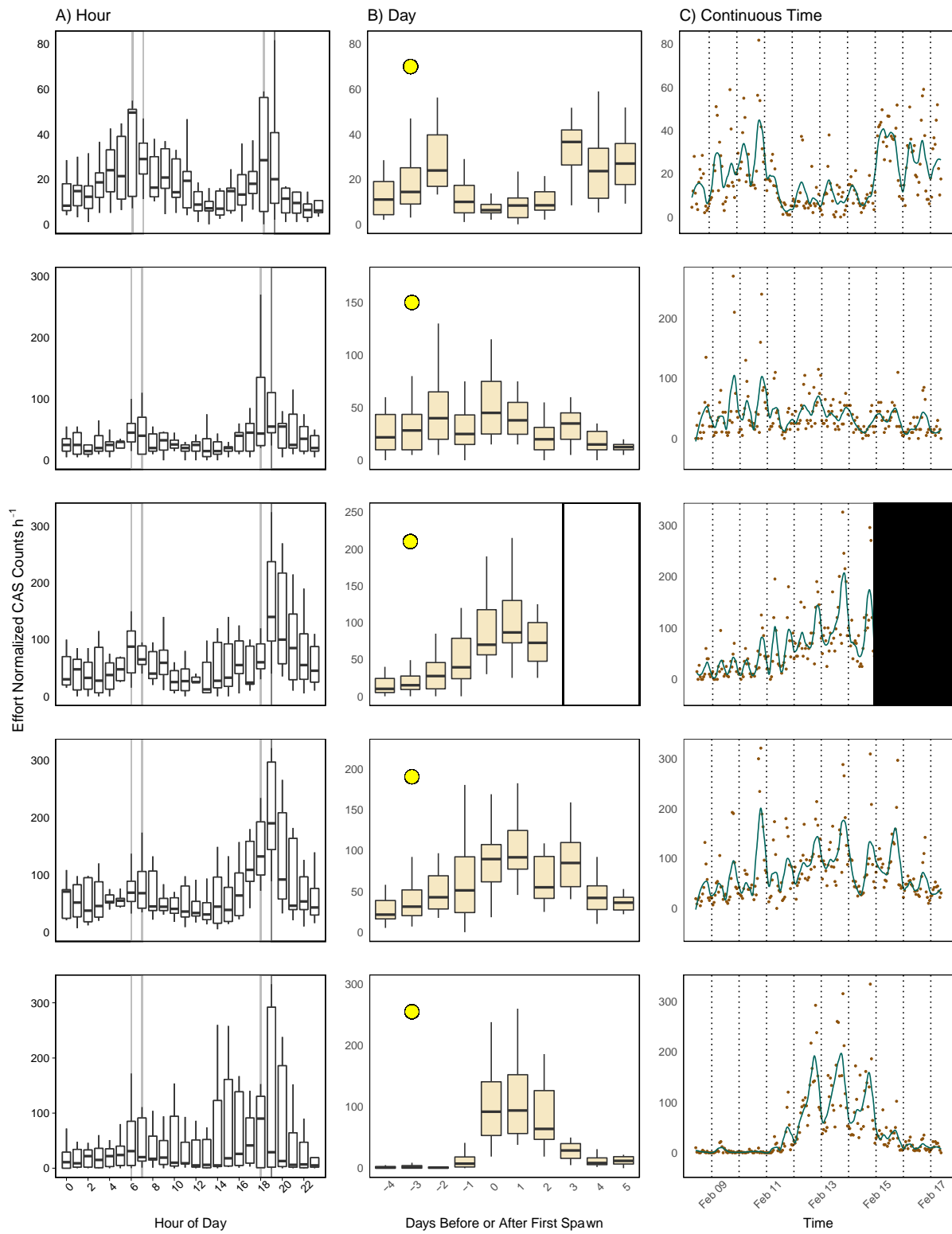
Station	Classifier	Cohen's Kappa	Accuracy	Misclassification Rate	True Positive Rate	True Negative Rate	False Positive Rate	False Negative Rate	Precision	Prevalence	Null Error Rate
LARSI	FADAR	69.5	88.0	12.0	63.4	99.5	0.5	36.6	98.5	31.9	31.9
	FADAR	11.6	47.8	52.2	13.2	1.0	0.0	86.8	1.0	60.2	39.8
ST2	HUMAN	67.0	83.8	16.2	82.9	85.0	15.0	17.1	88.5	58.3	41.7
	FADAR	5.1	58.1	41.9	4.4	1.0	0.0	95.6	1.0	43.8	43.8
ST4	HUMAN	66.0	84.1	15.9	81.2	90.6	9.4	18.8	95.1	68.9	31.1
	FADAR	61.5	82.8	17.2	80.6	88.9	11.1	19.4	95.2	73.3	26.7
ST6	FADAR	67.8	84.7	15.3	67.2	98.3	1.7	32.8	96.8	43.6	43.6

3.1 Spatiotemporal trends

Regardless of distance, all stations detected crepuscular patterns in Nassau calling rates (Figure 2A). Hours in which the sun rose or set had the highest average CAS frequencies per hour, specifically 06:00-08:00 and 18:00-20:00 (Figure 2A). All stations detected greater CAS calling rates in the evening hours compared to the morning, except for LARS1 which detected an equivalent share of CAS in both periods. ST6 had the highest variability of CAS calling rates as exemplified by low median rates and exceptionally high upper quartile ranges during most daylight hours. Hydrophones nearest to the FSA (ST4, LARS5, and ST6) detected CAS more frequently during days in which individuals spawned (0 to +2 DAFS; Figure 2B). On most days during the study period CAS frequencies showed crepuscular patterns across all hydrophones (Figure 2C). Both daylight and nighttime hours contained comparably low frequencies of CAS.

Proximal hydrophone pairs demonstrated higher correlations in CAS detections through time than distant pairs (Figure 3). Estimated correlation (ρ) decreased with increasing distance between pairs, ranging from 0.75 to -0.27 at separation distances of 122.6 m and 602.9 m, respectively (Figure 4). Correlation regressed over distance between pairs estimated correlation equaling zero at roughly 590 meters of separation between hydrophones (Figure 4). The comparison of ST4–LARS5 yielded the highest estimate of ρ (0.75) while other comparisons of adjacent hydrophones yielded estimates above 0.50. Despite being placed 262.0 m apart, ST4 and ST6 were found to have a high ρ estimate (0.73) – likely due to their positions on opposite sides of the aggregation.

Figure 2: Temporal trends of effort normalized Nassau Grouper CAS production rates across all hydrophones. Because ST4 abruptly halted recording at midnight of 3 DAFS, black rectangles cover 3-5 DAFS for ST4 in (B) and (C). (A) Box plots of CAS production rates for all hours of day at each hydrophone. Dark grey rectangles signify hours at night while light grey rectangles signify hours in which the sun rose (06:00) and set (18:00). (B) Box plots of CAS production rates averaged by day at each hydrophone. Yellow circles outlined black symbolize the full moon which occurred -3 DAFS. (C) CAS production rates for all continuous hours of observation. A green spline fits to the orange points by the loess method with a span factor of 0.1. The dark grey shade around the fitted spline represents the 89% confidence. Dotted black lines separate days.



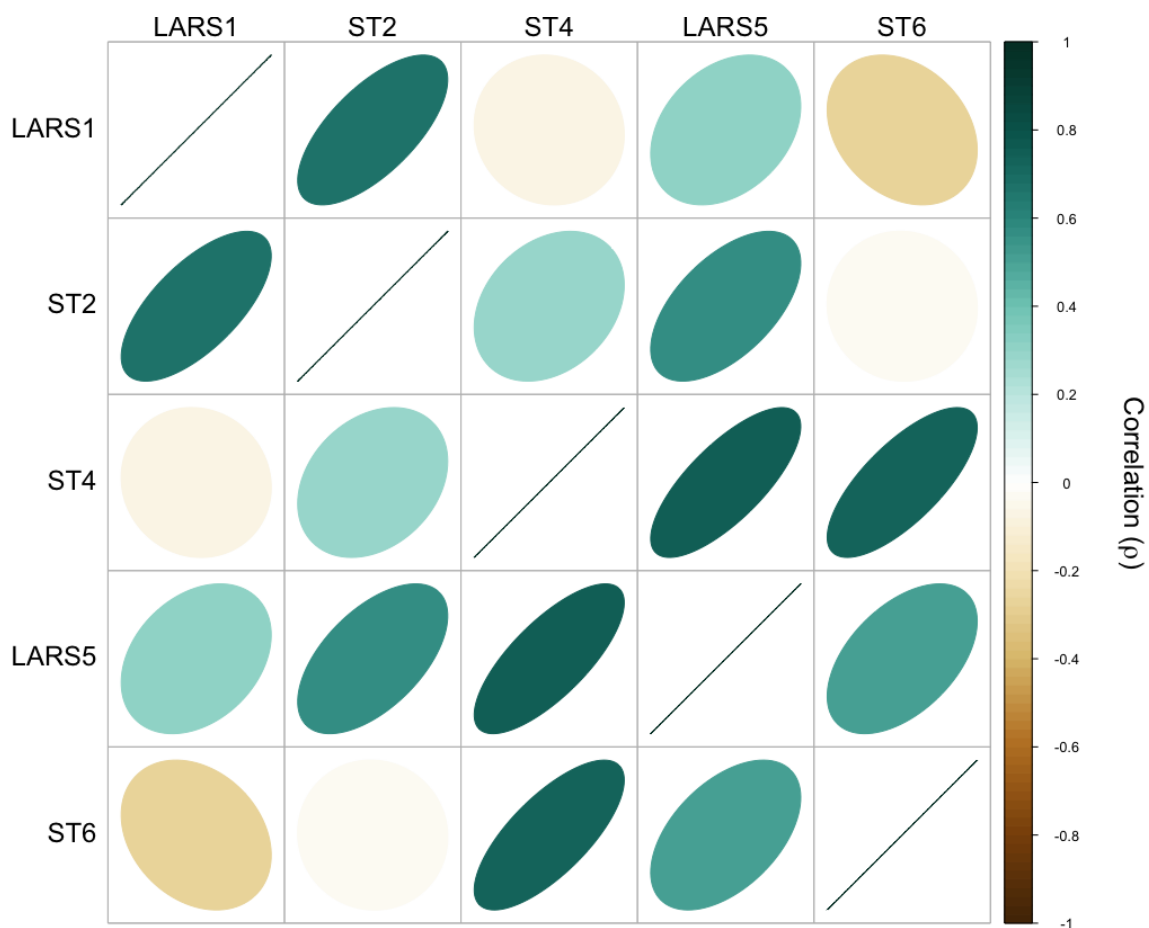


Figure 3: Correlation matrix plot of correlations among each hydrophone pair. The slope and color of the ellipses symbolize the strength of correlation (e.g. strong positive correlations are narrow ellipses angled positively and colored dark green). Straight, positively sloped lines occupy comparisons of identical pairs (e.g. LARS1-LARS1).

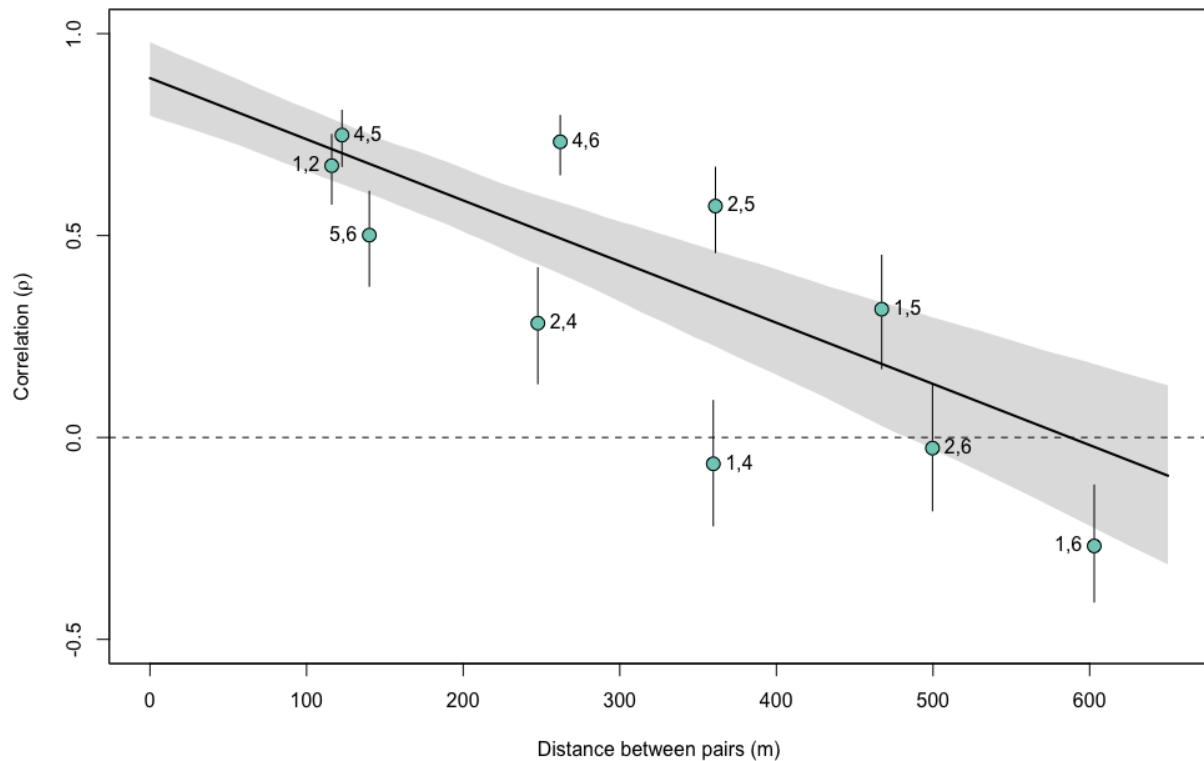


Figure 4: Linear regression of correlation coefficients against distance between hydrophone pairs in meters. Light green points symbolize the correlation coefficient of all hydrophone pairs at their distance of separation, with corresponding labels of the pair adjacent to each point. Whiskers extending from each point represent 95% confidence in the estimated coefficient. 95% confidence in the regression is highlighted in light grey.

3.2 Model

Time of day, day of spawning period, and proximity of the mass of fish to each hydrophone were all strong predictors of CAS rates (Figure 5). As with the correlation analysis, ST4's shorter recording period limited predictions to -4 to +2 DAFS. Model estimated Nassau Grouper CAS rates were higher during sunset (19:00) than sunrise (07:00) though there was small overlap in estimated 95% confidence intervals (Table A1). Crepuscular hours (defined as 06:00-08:59 and 18:00-20:59) had the highest estimated CAS rates. Nassau Groupers were least likely to produce CAS during the middle of the night (02:00) and day (13:00; Table A1).

Model estimated Nassau Grouper CAS rates increased from the first day of observation and peaked during spawning. The first day of observation, occurring just before the full moon and four days before spawning, had the lowest predicted Nassau Grouper CAS rates (-4 DAFS; Table A1). Estimated CAS rates increased from the first day of observation and peaked at 1 DAFS, though there was overlap in confidence intervals in both the prior and subsequent days (Table A1). Fish proximity to the hydrophone strongly predicted hydrophone-specific Nassau CAS detection rates. We considered other models with different predictors, such as current velocity, temperature, and hydrophone model, for their potential implications in Nassau spawning behavior thus CAS production (Colin 1992, Dahlgren et al. 2016). Comparisons using WAIC found these models to have weaker predictive ability than the model we selected for analysis.

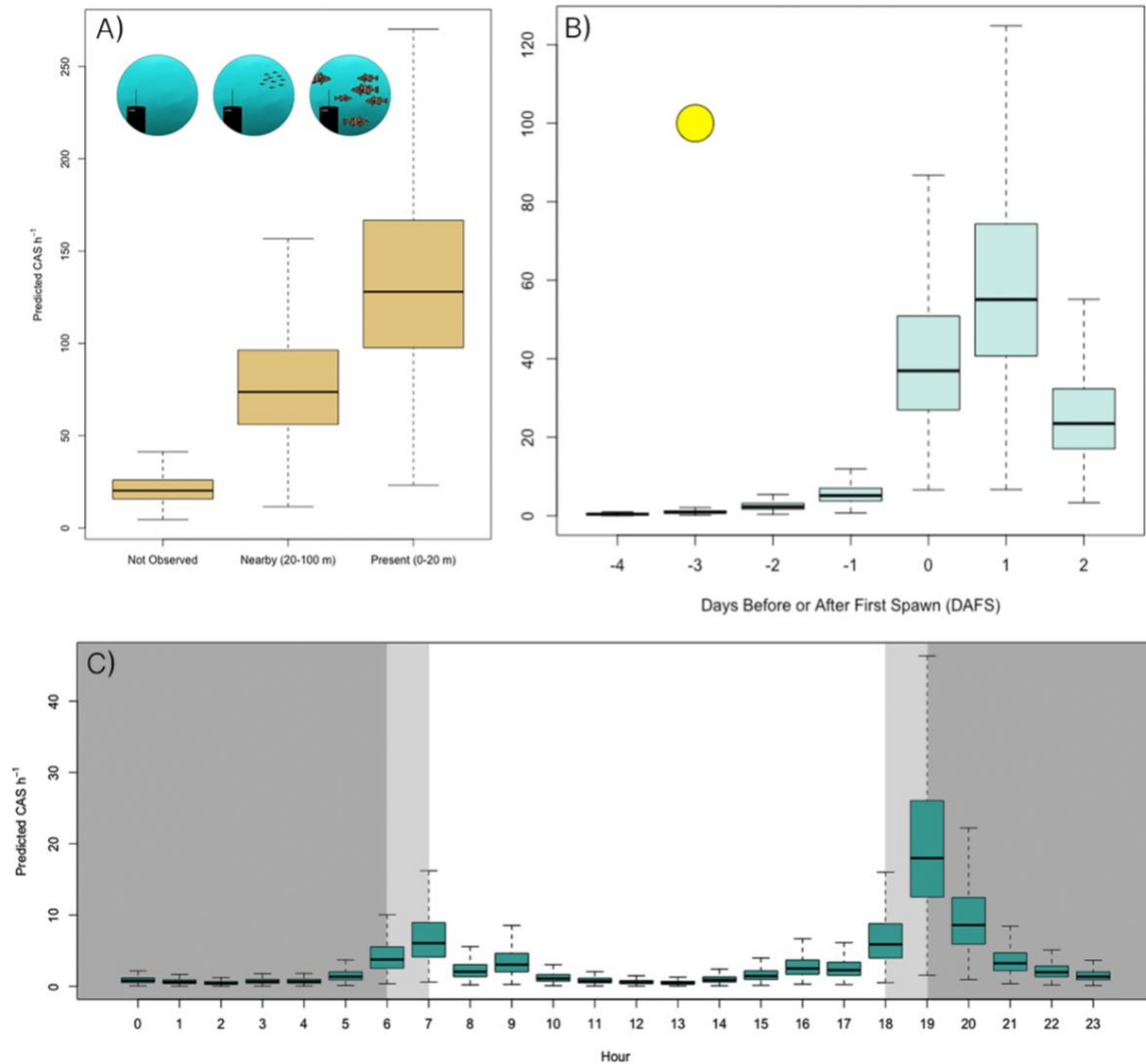


Figure 5: Box plots of posterior predictions of the parameters (A) T_i , (B) D_i , and (C) FP_i (see 2.4 for variable descriptions). (A) Posterior predictions of CAS production rates by T_i . Dark grey panels signify nighttime hours, with light grey panels representing the hours of sunrise (06:00) and sunset (18:00). (B) Posterior predictions of CAS production rates by D_i . A yellow circle outlined black signifies the full moon on -3 DAFS. (C) Posterior predictions of CAS production rates by FP_i . Cartoons roughly representing each category at the top of the panel jig slightly left for ease of viewing.

4. Discussion

Nearly all prior investigations into the temporal dynamics of spawning-related CAS sounds for Nassau Grouper and related tropical grouper species have relied on a single hydrophone deployment at or near the FSA. Given the potential for limited detection ranges relative to movements of fish at the spawning site (Schärer et al. 2012, Wilson et al. 2020), any temporal dynamics inferred from these studies at least partially reflect both temporal patterns in CAS and the movements of spawning fishes relative to the hydrophone. The goal of our study was to capture the spatial field of CAS across the spawning site per unit time, while simultaneously documenting dynamics in the location of spawning fish relative to each hydrophone in our array. By accounting for these spatial dynamics in our subsequent modeling efforts, we were able to quantify the influence of movement on CAS dynamics at the level of individual hydrophones. Moreover, we were able to separate the influence of spatial dynamics from the temporal dynamics in CAS (time of day, day of spawning period). The resulting estimates of temporal dynamics are thus uniquely “clean” estimates of temporal dynamics and rates of soniferous behaviors at the spawning site.

4.1. Nassau Grouper calling trends

While the change in raw CAS detection rates across days of the spawning period varied widely by individual hydrophone (Figure 2C), the model estimated average daily CAS detection rates across the array (after accounting for spatial dynamics in fish behavior) showed a gradual increase following the full moon and an exponential increase once fish began spawning, with a peak on the 2nd night of spawning.

The relationship of the winter full moon and Nassau Grouper spawning behavior in the Caribbean has been reported in the literature as early as 1972 (Smith), and there is general consensus that the winter lunar cycle is a key environmental cue in migratory and aggregating behaviors (Domeier & Colin 1997, Bolden 2000, Sala et al. 2001). While the drivers behind individuals' directed migrations to the FSA are unclear, there is evidence that first-time spawners follow more experienced fish, a behavior that may be mediated by sound production in older Nassau Groupers (Rowell et al. 2015, Dahlgren et al. 2016). The role of CAS in migration and spatial organization at the FSA appears to be evident in the CAS production rates observed at LARS1 and ST2. These hydrophones were the furthest to the Southeast (away from where the spawning ultimately occurred; Figure 1C) and recorded the highest CAS rates at the beginning and end of the spawning period, presumably when migrating fish were entering/leaving the spawning grounds. Conversely, those hydrophones closest to where the FSA formed (Figure 1C) recorded the highest rates of CAS on spawning days (Figure 2B). Collectively, the hydrophones appear to capture the temporal pattern of arrival, staging, and ultimately coalescing to spawn, all of which are reflected in CAS variability across space and time.

Nassau Grouper produced the highest CAS rates during nights of spawning. At hydrophones nearest to the aggregation, CAS production peaked from 0 to +2 DAFS, the same time frame in which divers observed spawning behavior (e.g. release of gametes into the water column). Nassau Grouper often produce the low-frequency tonal call while exhibiting courtship behavior, which can include body coloration shifts (Archer et al. 2012, Schärer et al. 2012). Tonal CAS are hypothesized to signal a readiness to mate among individuals, and to cue spawning synchrony for the greater population (i.e. FSA formation; Schärer et al. 2012). At the Little Cayman west end spawning site, peaks in tonal CAS occur as thousands of individuals

concentrate into a narrow band along a short section of the shelf break. In previous studies, researchers were unable to partition the rise in spawning-associated CAS rates due to the increased concentration of individuals versus increases in per capita CAS production. By accounting for the spatial distribution of fish at the spawning site across time in our model, we were able to approximately separate spatial effects of CAS rates from per capita CAS rates, and in so doing demonstrate that both factors mediate the detection rates of CAS at a given hydrophone.

Nassau Grouper exhibited increased CAS rates during crepuscular periods, regardless of the day of spawning period or where on the spawning grounds they were (near or far from the FSA). All hydrophone stations across the recording period recorded greater frequencies of CAS during dawn and dusk hours than all other times of day, with dusk typically containing the highest CAS density (Figure 2C). The increase in average CAS production rates during hours leading up to sunset likely reflects individuals signaling readiness to spawn. Throughout their range, Nassau Groupers spawn near sunset, presumably because this timing reduces egg predation (Colin 1992) and/or predation on spawning adults (e.g. Caribbean Reef Sharks at the study site, often observed attacking Nassau Grouper during gamete release). Overnight, simultaneous cross-shelf wind-driven currents help transport eggs on-shore to nursery habitat (Shenker et al. 1993). CAS production near dusk may be an evolutionary response to motivate spawning for high larval settlement. However, why would increases in CAS in crepuscular periods occur even well away from the FSA and outside nights of spawning? It seems likely that courtship behavior among individuals is protracted, occurring over multiple days and well before evenings of gamete release – in such a scenario, mate selection at spawning may result from many previous nights of pairwise interactions, particularly during evening periods when

individuals take on spawning colorations (Archer et al. 2012) that presumably reflect both fitness and readiness to spawn. Alternatively, CAS rates could increase during crepuscular periods simply because these time periods are when Nassau Grouper are most active (regardless of spawning season). Blincow et al. (2020) found Nassau Groupers were more likely to increase vertical swimming activity in dawn and dusk hours and linked this behavior to possible hunting strategies. Nassau Groupers are known to hunt in light-limited conditions as it benefits their ambush-style predation (Carter et al. 1994). Though there is no present evidence that links CAS to hunting behavior, Nassau Groupers do produce a pulse CAS (described as akin to a heartbeat; Rowell et al. 2018) during agonistic displays of defense for a mate. The novelty of this CAS and its ties to aggression suggest sound production may be used in hunting, perhaps to defend a territory well suited for ambush, though this is speculative.

4.2. Spatial variability

The location of hydrophones on the spawning grounds had a remarkably strong effect on the temporal variability in CAS detections. Simple correlation comparisons among hydrophone datasets indicate the potential for the acoustic picture of an FSA to fully invert (highest CAS rates outside nights of peak spawning) if the distance between a hydrophone and the FSA exceeds only several hundred meters. While the time of day and spawning behavior by Nassau Grouper drove CAS production, fish presence near a hydrophone strongly influenced CAS detection rates, suggesting variability in fish movement around an FSA can severely impact temporal acoustic trends. Our results indicate a clear need for future studies to either verify the proximities of fish near the recording hydrophone or alternatively implement a hydrophone array that captures spatio-temporal variability across the spawning grounds. This is particularly true if

researchers intend to compare CAS rates across spawning seasons or between spawning grounds – that is, unless the spatial effects of CAS rates we document here are accounted for in studies seeking to approximate spawner abundance (relative or absolute), the resulting findings are likely to be hopelessly compromised.

Perhaps unsurprisingly, we found a strong decay in CAS detection rate correlations between hydrophones as a function of distance. Previous studies have suggested that the detection range of Nassau Grouper CAS at a particular hydrophone is roughly 200 meters (Schärer et al. 2012, Wilson et al. 2020). Our findings generally support this range. Moreover, at a distance of 300 meters, correlations between our hydrophone detections became negative, a reflection of strong, small-scale spatial patterns in CAS rates on the spawning grounds. From a monitoring perspective, the interactive effects of limited detection ranges and relatively fine-scale acoustic behaviors mean that hydrophone placements are a critically important part of efforts to capture spawning dynamics and spawner abundance.

FSA's are typically thought of as fixed, immutable locations that afford opportunities for population assessment that otherwise might be cost-prohibitive or impossible given low densities of some aggregating species when they are on their home reefs. However, mounting evidence suggests that the spatial nature of aggregations is dynamic at scales ranging from 100s of meters to 10s of km or more (Colin 1992, Aguilar-Perera 2006, Caiger et al. 2020). The Nassau Grouper FSA we targeted is no exception; during our study, we observed individuals several hundred meters north of the traditional FSA location (based on previous years of FSA monitoring; Figure 1C). Because this shift in FSA location was larger than the apparent range of any given hydrophone, we captured trends in CAS rates on ST2 (the functional hydrophone nearest the traditional FSA site) that were not representative of the true trends in CAS rates across the

spawning period – naively, such a finding in the absence of diver observations might be interpreted as evidence of spawning failure. More generally, CAS patterns coupled with a weaker correlation among hydrophones nearer to the historic FSA compared to hydrophones nearer to the observed FSA suggest reliance on past estimates of FSA locations can introduce greater uncertainty in recorded data.

The diver and GoPro estimated abundance of Nassau Grouper within 20 to 100 meters of a given hydrophone was a strong predictor of recorded CAS rates for that hydrophone. In fact, regardless of time of day or day of spawning season, when the aggregation of fish was within 20m of a hydrophone (present), CAS rates were approximately 10 times as high as when fish were not visibly present near a hydrophone (not observed; Figure 5A). This finding provides strong evidence that the movements of fish around the spawning grounds, on the scale of hours to days, can have dramatic impacts on hydrophone-specific CAS detection rates that are unrelated to the tendencies of individual fish to call more or less frequently as a function of time. Why might this matter from a monitoring perspective? Even when researchers deploy an array of hydrophones to address spatial variance in calling frequencies, if unobserved fish movements at the spawning site are synchronized to temporal patterns of interest (e.g. the FSA moves in close proximity to a specific hydrophone each evening), spatial movements may erroneously be interpreted as temporal changes in CAS rates in subsequent modeling efforts. At a minimum, researchers should be aware of this potential confounding effect in future studies. Should time and support allow, we recommend pairing some amount of visual monitoring (*in situ* or with imaging technologies) in order to help parse the relative effects of time and space in driving CAS rates.

The spectral structures of CAS and other biotic sounds are species-specific, which enables researchers to distinguish between calls of several taxa. Particularly in tropical systems, FSAs can be composed of multiple soniferous species that have temporally overlapping spawning periods. Our study site is an example of such multi-species FSAs as it is the spawning ground for several other soniferous grouper species, including (Red Hind (*E. guttatus*), Yellowfin Grouper (*Mycteroperca venenosa*), and Black Grouper (*M. bonaci*)). The CAS of these groupers share spectral qualities with that of Nassau Grouper, which, coupled with spatial overlap of aggregating behaviors, can contribute to a noisy soundscape that partially masks target CAS (Wilson et al. 2020). Sonic interference can occur from anthropogenic sources as well. As we observed in our data, motorized vessels create loud, long-lasting sounds at low frequencies that overlap with CAS of several fish species and can thus prevent detection (Webb et al. 2008). As with the potential for spatial movement patterns to generate spurious trends in CAS rates, biogenic or anthropogenic interference may also alter patterns in CAS rates.

The presumptive spatiotemporal predictability of FSAs and use of CAS by aggregating species has resulted in the broad adoption of PAM as an efficient, cost-effective tool to collect data on aggregating populations. However, turning the acoustic recordings these tools generate into metrics that reflect metrics of stock status has proven challenging. By using an array of hydrophones and monitoring the location of aggregating fishes in relation to these hydrophones across time, we were able to partition the competing effects of time, space and behaviors on CAS rates. Understanding each of these effects and their collective influence on CAS detections at a given hydrophone is a necessary step in effort to get CAS rates as a function of population size. It is thus recommended that any study focused on inferring ecological behaviors and distributions of a soniferous species should report, or acknowledge uncertainty in, the separation

between the sound source and the receiver. Otherwise, substantial error from imprecise methods may significantly misrepresent a species' ecology and reduce the efficacy of subsequently informed management actions.

Appendix

Equation A1: Calculate classifier accuracy (A) from true positive (TP), true negative (TN), and total (n) parameters. Misclassification rate (MCR) can be found by subtracting A from 1.

$$A = \frac{(TP + TN)}{n}$$

Equation A2: Calculate True Positive Rate (or recall; TPR) from true positive (TP) and actual presence (AP) parameters. False Negative Rate (TNR) can be found by subtracting TPR from 1.

$$TPR = \frac{TP}{AP}$$

Equation A3: Calculate False Positive Rate (FPR) from false positive (FP) and actual absence (AA) parameters. True Negative Rate (TNR) can be found by subtracting FPR from 1.

$$FPR = \frac{FP}{AA}$$

Equation A4: Calculate Cohen's Kappa (K) from true positive (TP), true negative (TN), false negative (FN), and false positive (FP) parameters.

$$K = 2 * \frac{(TP * TN) - (FN * FP)}{((TP + FP) * (FP + TN)) + ((TP + FN) * (FN + TN))}$$

Table A3: Results of Bayesian mixed effects model for modeling CAS rates by hour of day, day of spawning period, and fish proximity to a given hydrophone. Bolded data points reflect local maximums in posterior means. Data and model code can be found at <https://github.com/cjvanhorn>.

Parameter	Posterior Mean (Log CAS/hr)	95% Confidence Interval	
		Lower	Upper
0:00	-0.256	-1.404	0.917
1:00	-0.523	-1.735	0.720
2:00	-0.838	-2.052	0.320
3:00	-0.416	-1.599	0.745
4:00	-0.419	-1.502	0.746
5:00	0.296	-0.862	1.526
6:00	1.283	0.117	2.382
7:00	1.809	0.617	2.972
8:00	0.729	-0.508	1.902
9:00	1.154	0.025	2.366
10:00	0.108	-1.072	1.281
11:00	-0.294	-1.379	0.878
12:00	-0.621	-1.722	0.539
13:00	-0.783	-1.954	0.350
14:00	-0.103	-1.237	1.082
15:00	0.365	-0.825	1.491
16:00	0.903	-0.228	2.011
17:00	0.822	-0.297	1.875
18:00	1.798	0.622	2.937
19:00	2.852	1.797	3.929
20:00	2.116	1.031	3.232
21:00	1.166	0.115	2.268
22:00	0.657	-0.425	1.702
23:00	0.283	-0.805	1.348
-4 DAFS	-1.005	-2.134	0.102
-3 DAFS	-0.115	-1.094	0.797
-2 DAFS	0.840	-0.086	1.680
-1 DAFS	1.642	0.742	2.492
0 DAFS	3.626	2.739	4.534
1 DAFS	4.007	3.191	4.859
2 DAFS	3.147	2.272	4.085
Not Observed	3.004	2.328	3.664
Nearby	4.315	3.590	5.014
Present	4.858	4.139	5.559

References

- Aalbers, S.A., Sepulveda, C.A., 2012. The utility of a long-term acoustic recording system for detecting white seabass *Atractoscion nobilis* spawning sounds. *Journal of Fish Biology* 81, 1859–1870. <https://doi.org/10.1111/j.1095-8649.2012.03399.x>
- Aguilar-Perera, A., 2006. Disappearance of a Nassau grouper spawning aggregation off the southern Mexican Caribbean coast. *Mar. Ecol. Prog. Ser.* 327, 289–296. <https://doi.org/10.3354/meps327289>
- Archer, S.K., Heppell, S.A., Semmens, B.X., Pattengill-Semmens, C.V., Bush, P.G., McCoy, C.M., Johnson, B.C., 2012. Patterns of color phase indicate spawn timing at a Nassau grouper *Epinephelus striatus* spawning aggregation. *Current Zoology* 58, 73–83. <https://doi.org/10.1093/czoolo/58.1.73>
- Blinchow, K., Bush, P., Heppell, S., McCoy, C., Johnson, B., Pattengill-Semmens, C., Heppell, S., Stevens-McGeever, S., Whaylen, L., Luke, K., Semmens, B., 2020. Spatial ecology of Nassau Grouper at home reef sites: using acoustic telemetry to track a large, long-lived epinephelid across multiple years (2005–2008). *Mar. Ecol. Prog. Ser.* 655, 199–214. <https://doi.org/10.3354/meps13516>
- Bolden, S.K., 2000. Long-distance movement of a Nassau grouper (*Epinephelus striatus*) to a spawning aggregation in the central Bahamas. *Fish Bull* 98, 642–645.
- Bush, P.G., Lane, E.D., Ebanks-Petrie, G.C., Luke, K., Johnson, B., McCoy, C., Bothwell, J., Parsons, E., 2006. The Nassau Grouper Spawning Aggregation Fishery of the Cayman Islands – An Historical and Management Perspective. *Gulf and Caribbean Fisheries Institute* 57, 515–524.
- Caiger, P., Dean, M., DeAngelis, A., Hatch, L., Rice, A., Stanley, J., Tholke, C., Zemeckis, D., Van Parijs, S., 2020. A decade of monitoring Atlantic cod *Gadus morhua* spawning aggregations in Massachusetts Bay using passive acoustics. *Mar. Ecol. Prog. Ser.* 635, 89–103. <https://doi.org/10.3354/meps13219>
- Carter J, Marrow G, Pryor V, 1994. Aspects of the ecology and reproduction of Nassau grouper (*Epinephelus striatus*) off the coast of Belize, Central America. *Proc Gulf Caribb Fish Inst* 43:65–111
- Colin, P.L., 1992. Reproduction of the Nassau grouper, *Epinephelus striatus* (Pisces: Serranidae) and its relationship to environmental conditions. *Environ Biol Fish* 34, 357–377. <https://doi.org/10.1007/BF00004740>
- Dahlgren, C.P., Buch, K., Rechisky, E., Hixon, M.A., 2016. Multiyear Tracking of Nassau Grouper Spawning Migrations. *Marine and Coastal Fisheries* 8, 522–535. <https://doi.org/10.1080/19425120.2016.1223233>

- De Mitcheson, Y.S., Cornish, A., Domeier, M., Colin, P.L., Russell, M., Lindeman, K.C., 2008. A Global Baseline for Spawning Aggregations of Reef Fishes. *Conservation Biology* 22, 1233–1244. <https://doi.org/10.1111/j.1523-1739.2008.01020.x>
- Domeier, M.L., Colin, P.L., 1997. Tropical Reef Fish Spawning Aggregations: Defined and Reviewed. *Bulletin of Marine Science* 60, 698–726.
- Emslie, M.J., Cheal, A.J., MacNeil, M.A., Miller, I.R., Sweatman, H.P.A., 2018. Reef fish communities are spooked by scuba surveys and may take hours to recover. *PeerJ* 6, e4886. <https://doi.org/10.7717/peerj.4886>
- FAO. 2020. The State of World Fisheries and Aquaculture 2020. Sustainability in action. Rome. <https://doi.org/10.4060/ca9229en>
- Heppell, S. A., Semmens, B. X., Pattengill-Semmens, C. V., Bush, P. G., Johnson, B. C., McCoy, C. M., Paris, C., Gibb, J., Heppell, S.S., 2009. Tracking potential larval dispersal patterns from Nassau grouper aggregation sites: Evidence for local retention and the “importance of place”. In *Proceedings of the 61st Gulf and Caribbean Fisheries Institute*, pp. 325–327. Gosier, Guadeloupe, French West Indies.
- Heppell, S.A., Semmens, B.X., Archer, S.K., Pattengill-Semmens, C.V., Bush, P.G., McCoy, C.M., Heppell, S.S., Johnson, B.C., 2012. Documenting recovery of a spawning aggregation through size frequency analysis from underwater laser calipers measurements. *Biological Conservation* 155, 119–127. <https://doi.org/10.1016/j.biocon.2012.06.002>
- Ibrahim, A.K., Zhuang, H., Chérubin, L.M., Schärer-Umpierre, M.T., Erdol, N., 2018. Automatic classification of grouper species by their sounds using deep neural networks. *The Journal of the Acoustical Society of America* 144, EL196–EL202. <https://doi.org/10.1121/1.5054911>
- Laiolo, P., 2010. The emerging significance of bioacoustics in animal species conservation. *Biological Conservation* 143, 1635–1645. <https://doi.org/10.1016/j.biocon.2010.03.025>
- Lindseth, A., Lobel, P., 2018. Underwater Soundscape Monitoring and Fish Bioacoustics: A Review. *Fishes* 3, 36. <https://doi.org/10.3390/fishes3030036>
- Lobel, P.S., 1992. Sounds produced by spawning fishes. *Environmental Biology of Fishes* 33, 351–358.
- Looby, A., Cox, K., Bravo, S., Rountree, R., Juanes, F., Reynolds, L.K., Martin, C.W., 2022. A quantitative inventory of global soniferous fish diversity. *Rev Fish Biol Fisheries* 32, 581–595. <https://doi.org/10.1007/s11160-022-09702-1>
- Luczkovich, J.J., Mann, D.A., Rountree, R.A., 2008. Passive Acoustics as a Tool in Fisheries Science. *Transactions of the American Fisheries Society* 137, 533–541. <https://doi.org/10.1577/T06-258.1>

- Mann, D.A., Hawkins, A.D., Michael, Jech, J.M., 2008. Active and Passive Acoustics to Locate and Study Fish. In: Fish Bioacoustics. (eds. J.F. Webb, A.N. Popper, and R.R. Fay). Springer, New York, pp. 279-309.
- Marques, T.A., Thomas, L., Martin, S.W., Mellinger, D.K., Ward, J.A., Moretti, D.J., Harris, D., Tyack, P.L., 2013. Estimating animal population density using passive acoustics. *Biol Rev* 88, 287–309. <https://doi.org/10.1111/brv.12001>
- McElreath R (2020). *_rethinking: Statistical Rethinking book package_*. R package version 2.01
- Milich, L., 1999. Resource Mismanagement Versus Sustainable Livelihoods: The Collapse of the Newfoundland Cod Fishery. *Society & Natural Resources* 12, 625–642. <https://doi.org/10.1080/089419299279353>
- Monczak, A., Ji, Y., Soueidan, J., Montie, E.W., 2019. Automatic detection, classification, and quantification of sciaenid fish calls in an estuarine soundscape in the Southeast United States. *PLoS ONE* 14, e0209914. <https://doi.org/10.1371/journal.pone.0209914>
- Munger, J., Herrera, D., Haver, S., Waterhouse, L., McKenna, M., Dziak, R., Gedamke, J., Heppell, S., Haxel, J., 2022. Machine learning analysis reveals relationship between pomacentrid calls and environmental cues. *Mar. Ecol. Prog. Ser.* 681, 197–210. <https://doi.org/10.3354/meps13912>
- Nemeth, R.S., 2012. Ecosystem Aspects of Species That Aggregate to Spawn. In: Sadovy de Mitcheson, Y., Colin, P. (eds) Reef Fish Spawning Aggregations: Biology, Research and Management. Fish & Fisheries Series, vol 35. https://doi.org/10.1007/978-94-007-1980-4_2
- Rountree, R.A., Gilmore, R.G., Goudey, C.A., Hawkins, A.D., Luczkovich, J.J., Mann, D.A., 2006. Listening to Fish: Applications of Passive Acoustics to Fisheries Science. *Fisheries* 31, 433–446. [https://doi.org/10.1577/1548-8446\(2006\)31\[433:LTF\]2.0.CO;2](https://doi.org/10.1577/1548-8446(2006)31[433:LTF]2.0.CO;2)
- Rowell, T., Nemeth, R., Schärer, M., Appeldoorn, R., 2015. Fish sound production and acoustic telemetry reveal behaviors and spatial patterns associated with spawning aggregations of two Caribbean groupers. *Mar. Ecol. Prog. Ser.* 518, 239–254. <https://doi.org/10.3354/meps11060>
- Rowell, T., Schärer, M., Appeldoorn, R., Nemeth, M., Mann, D., Rivera, J., 2012. Sound production as an indicator of red hind density at a spawning aggregation. *Mar. Ecol. Prog. Ser.* 462, 241–250. <https://doi.org/10.3354/meps09839>
- Rowell, T.J., Demer, D.A., Aburto-Oropeza, O., Cota-Nieto, J.J., Hyde, J.R., Erisman, B.E., 2017. Estimating fish abundance at spawning aggregations from courtship sound levels. *Sci Rep* 7, 3340. <https://doi.org/10.1038/s41598-017-03383-8>

- Rowell, T.J., Schärer, M.T., Appeldoorn, R.S., 2018. Description of a New Sound Produced by Nassau Grouper at Spawning Aggregation Sites. GCR 29, GCFI22–GCFI26. <https://doi.org/10.18785/gcr.2901.12>
- Sadovy, Y., Aguilar-Perera, A. & Sosa-Cordero, E. 2018. *Epinephelus striatus*. The IUCN Red List of Threatened Species 2018: e.T7862A46909843.
- Sadovy, Y. and Eklund, A.M., 1999. Synopsis of biological data on the Nassau grouper, *Epinephelus striatus* (Bloch, 1792), and the jewfish, *E. itajara* (Lichtenstein, 1822). NOAA Technical Report NMFS No. 146. NOAA/National Marine Fisheries Service, Seattle, WA, pp. 65.
- Sala, E., Ballesteros, E., Starr, R.M., 2001. Rapid Decline of Nassau Grouper Spawning Aggregations in Belize: Fishery Management and Conservation Needs. *Fisheries* 26, 8.
- Sanchez, P.J., Appeldoorn, R.S., Schärer-Umpierre, M.T., Locascio, J.V., 2017. Patterns of courtship acoustics and geophysical features at spawning sites of black grouper (*Mycteroperca bonaci*). *FB* 115, 186–195. <https://doi.org/10.7755/FB.115.2.5>
- Schärer, M., Rowell, T., Nemeth, M., Appeldoorn, R., 2012. Sound production associated with reproductive behavior of Nassau grouper *Epinephelus striatus* at spawning aggregations. *Endang. Species. Res.* 19, 29–38. <https://doi.org/10.3354/esr00457>
- Semmens, B.X., Luke, K.E., Bush, P.G., Pattengill-Semmens, C., Johnson, B., McCoy, C., Heppell, S., 2007. Investigating the Reproductive Migration and Spatial Ecology of Nassau grouper (*Epinephelus striatus*) on Little Cayman Island using Acoustic Tags – An Overview. *Gulf and Caribbean Fisheries Institute* 58, 191–198.
- Shenker, J., Maddox, E., Wishinski, E., Pearl, A., Thorrold, S., Smith, N., 1993. Onshore transport of settlement-stage Nassau grouper *Epinephelus striatus* and other fishes in Exuma Sound, Bahamas. *Mar. Ecol. Prog. Ser.* 98, 31–43. <https://doi.org/10.3354/meps098031>
- Smith, C.L., 1972. A Spawning Aggregation of Nassau Grouper, *Epinephelus striatus* (Bloch). *Transactions of the American Fisheries Society* 101, 257–261. [https://doi.org/10.1577/1548-8659\(1972\)101<257:ASAONG>2.0.CO;2](https://doi.org/10.1577/1548-8659(1972)101<257:ASAONG>2.0.CO;2)
- Stan Development Team. 2022. Stan Modeling Language Users Guide and Reference Manual, Version 2.31. <https://mc-stan.org>
- Starr, R., Sala, E., Ballesteros, E., Zabala, M., 2007. Spatial dynamics of the Nassau grouper *Epinephelus striatus* in a Caribbean atoll. *Mar. Ecol. Prog. Ser.* 343, 239–249. <https://doi.org/10.3354/meps06897>
- Stock, B.C., Heppell, S.A., Waterhouse, L., Dove, I.C., Pattengill-Semmens, C.V., McCoy, C.M., Bush, P.G., Ebanks-Petrie, G., Semmens, B.X., 2021. Pulse recruitment and recovery of Cayman Islands Nassau Grouper (*Epinephelus striatus*) spawning aggregations revealed

- by *in situ* length-frequency data. ICES Journal of Marine Science 78, 277–292.
<https://doi.org/10.1093/icesjms/fsaa221>
- Stowell, D., Petrusková, T., Šálek, M., Linhart, P., 2019. Automatic acoustic identification of individuals in multiple species: improving identification across recording conditions. J. R. Soc. Interface. 16, 20180940. <https://doi.org/10.1098/rsif.2018.0940>
- Teh, L.C.L., Sumaila, U.R., 2013. Contribution of marine fisheries to worldwide employment: Global marine fisheries employment. Fish and Fisheries 14, 77–88.
<https://doi.org/10.1111/j.1467-2979.2011.00450.x>
- Waterhouse, L., Heppell, S.A., Pattengill-Semmens, C.V., McCoy, C., Bush, P., Johnson, B.C., Semmens, B.X., 2020. Recovery of critically endangered Nassau grouper (*Epinephelus striatus*) in the Cayman Islands following targeted conservation actions. Proc. Natl. Acad. Sci. U.S.A. 117, 1587–1595. <https://doi.org/10.1073/pnas.1917132117>
- Whaylen, L., Bush, P., Johnson, B., Luke, K.E., McCoy, C., Semmens, B., Boardman, M., 2007. Aggregation dynamics and lessons learned from five years of monitoring at a Nassau grouper (*Epinephelus striatus*) spawning aggregation in Little Cayman, Cayman Islands, BWI. Gulf and Caribbean Fisheries Institute 59, 413–422.
- Whaylen, L., Pattengill-Semmens, C.V., Semmens, B.X., Bush, P.G., Boardman, M.R., 2004. Observations of a Nassau grouper, *Epinephelus striatus*, Spawning Aggregation Site in Little Cayman, Cayman Islands, Including Multi-Species Spawning Information. Environmental Biology of Fishes 70, 305–313.
<https://doi.org/10.1023/B:EBFI.0000033341.57920.a8>
- Wilson, K., Semmens, B., Pattengill-Semmens, C., McCoy, C., McCoy, C., 2020. Potential for grouper acoustic competition and partitioning at a multispecies spawning site off Little Cayman, Cayman Islands. Mar. Ecol. Prog. Ser. 634, 127–146.
<https://doi.org/10.3354/meps13181>
- Winemiller, K.O., Rose, K.A., 1992. Patterns of Life-History Diversification in North American Fishes: implications for Population Regulation. Can. J. Fish. Aquat. Sci. 49, 2196–2218.
<https://doi.org/10.1139/f92-242>
- Worm, B., Branch, T.A., 2012. The future of fish. Trends in Ecology and Evolution 27(11), 594–599. <https://doi.org/10.1016/j.tree.2012.07.005>.